Journal of Fluorine Chemistry 137 (2012) 54–63

Contents lists available at SciVerse ScienceDirect

Journal of Fluorine Chemistry

journal homepage: www.elsevier.com/locate/fluor

Synthesis and characterization of polyfluorinated 2,2′-bipyridines and their palladium and platinum complexes, [MX_2(bis($R_fCH_2OCH_2$)-2,2′-bpy)] (X = Cl, Br)

Norman Lu [a,*], Yu-Meng Ou [a,b], Tsung-Yao Feng [a,b], Wei-Jen Cheng [a,b], Wen-Han Tu [a], Han-Chang Su [a], Xiao Wang [b], Liu Liu [b], Matthew D. Hennek [b], Todd S. Sayler [b], Joseph S. Thrasher [b,c]

[a] Institute of Organic and Polymeric Materials, National Taipei University of Technology, Taipei 106, Taiwan
[b] Department of Chemistry, The University of Alabama, Tuscaloosa, AL 35487, USA
[c] Department of Chemistry, Clemson University, Advanced Materials Research Laboratory, Anderson, SC 29625, USA

ARTICLE INFO

Article history:
Received 5 November 2011
Received in revised form 10 February 2012
Accepted 16 February 2012
Available online 25 February 2012

Keywords:
Fluorous
Ponytails
X-ray diffraction studies
Hydrogen bond system
Chemical ionization (CI)

ABSTRACT

The fluorous-ponytailed bpy ligands at 4,4′ and 5,5′-positions, 4,4′-bis($R_fCH_2OCH_2$)-2,2′-bpy and 5,5′-bis($R_fCH_2OCH_2$)-2,2′-bpy, were prepared. Then these two differently positioned bpy ligands with varying fluorous lengths were treated with [$PdCl_2(CH_3CN)_2$], [$PtCl_2(CH_3CN)_2$], or the simple $PtBr_2$ salt to result in the corresponding 4,4′- or 5,5′-metal halide-containing complexes, [MX_2(bis($R_fCH_2OCH_2$)-2,2′-bpy)] [M = Pd or Pt; X = Cl or Br]. All of these ligands and metal complexes were fully characterized by multi-nuclei NMR (^1H, ^{19}F, and ^{13}C) and FTIR spectroscopy and mass spectrometry (GC/MS, EI and CI, or FAB). Additionally, single crystals of the Pd and Pt complexes with two bpy ligands were successfully obtained, and their X-ray structures are compared with their analogues.

1. Introduction

The Pd-catalyzed Heck reaction has become one of the most important reactions in developing styrene-type compounds, new drugs, biologically active compounds, and many other industrially useful chemicals or materials [1,2]. A number of applications of this reaction have been developed at both the laboratory and commercial levels. In particular, the scientist R.F. Heck won the Nobel Prize in 2010 with E.I. Negishi and A. Suzuki for this important discovery [3]. So far most of the efforts in the Pd-catalyzed Heck reaction have dealt with non-fluorine-containing Pd catalysts, substrates, products, mechanisms, etc. [4–6], but the development of an efficient and recyclable reaction system for the Heck reaction is still rare [7]. It has been shown that the incorporation of a fluorous segment into a metal system is one of the best ways to reach the efficiency and recyclability of the catalyst [8]. As for Pt complexes, their two main applications are known to be in medicinal chemistry [9] and optoelectronics [10]. Recently, we found that the cisplatin analogues of Pt–diimine complexes with or without the fluorous segments behave differently with respect to cytotoxicity [11]. The ability of the former to kill cancer cells turned out to be better than those of the latter. The optoelectronic properties of Pt complexes have also been widely studied [10], and it can be expected that Pt complexes with fluorous bpy ligands might give rise to some different emission properties resulting from their usual bonding properties in the solid state. Furthermore, this type of polyfluorinated bpy ligands has also been used to prepare novel fluorinated Ru complexes in order to tune the electron density and electrochemical property on the metal center [12–14]. The resulting Ru-based dye complexes, carrying fluorous-ponytailed bpy ligands, have been found to enhance both the efficiency and the chemical and thermal stability of the dyes [15] in solar cell tests. Therefore, the elucidation of the four structures of the Pd and Pt complexes of two different fluorous bpy ligands reported in this study could contribute not only to an already rich chemistry [2,16], but also to a better understanding of the related optoelectronic properties for likely extensions to organic light-emitting devices (OLEDs) [17] and solar cell research [18–21].

In the past few years, we have successfully synthesized a new class of bis($R_fCH_2OCH_2$)-2,2′-bpy ligands carrying fluorous ponytails at the 4,4′- or 5,5′-positions [22–25]. These ligands with long fluorous ponytails at the 4,4′-positions have been applied to recycle and reuse Pd-based catalysts under either fluorous biphasic (FB), thermomorphic, or $scCO_2$ conditions [25–29]. In this study, the fluorous ligands and their Pd or Pt complexes with shorter lengths of fluorous ligands at the 4,4′- and 5,5′-positions were prepared and spectroscopically characterized. Their chemical

* Corresponding author. Tel.: +886 2 2771 2171; fax: +886 2 2731 7174.
E-mail address: normanlu@ntut.edu.tw (N. Lu).

0022-1139/$ – see front matter © 2012 Elsevier B.V. All rights reserved.
doi:10.1016/j.jfluchem.2012.02.009

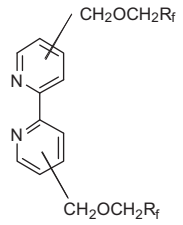

Substituent= $CH_2OCH_2R_f$

$CH_2OCH_2R_f$ at (1) 4,4' positions; when $R_f = CF_3$ (**1a**), C_2F_5 (**1b**), C_3F_7 (**1c**), $C_6F_{12}H$ (**1d**);

(2) 5,5' positions; when $R_f = CF_3$ (**2a**), C_2F_5 (**2b**), C_3F_7 (**2c**), $C_6F_{12}H$ (**2d**).

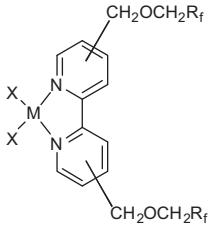

$CH_2OCH_2R_f$ at (3) 4,4' positions and M=Pd, X= Cl; when $R_f = CF_3$ (**3a**), C_2F_5 (**3b**), C_3F_7 (**3c**);

(4) 5,5' positions and M=Pd, X= Cl; when $R_f = CF_3$ (**4a**), C_2F_5 (**4b**);

(5) 4,4' positions and M=Pt, X= Cl; when $R_f = CF_3$ (**5a**), C_2F_5 (**5b**);

(6) 5,5' positions and M=Pt, X= Br; when $R_f = CF_3$ (**6a**).

Fig. 1. The chemical structures and numbering of all relevant polyfluorinated bpy ligands and their metal complexes.

structures and the relevant numbering of all polyfluorinated bpy ligands are shown in Fig. 1. Also reported are the X-ray structures of two single crystals of the Pd complexes, **3a** and **4a**, and two single crystals of the Pt complexes, **5a** and **6a**, along with structural comparisons and discussion.

2. Results and discussion

2.1. Synthesis

The preparation of ligand **1a** or **1c** was reported by us before [22,24]. A single general procedure for preparing this type of fluorous bpy ligands at 4,4′- and 5,5′- are described in detail in the experimental section. The fluorinated alcohols – e.g. $CF_3(CF_2)_2CH_2OH$, $HCF_2(CF_2)_5CH_2OH$ etc., were normally treated with 30% CH_3ONa/CH_3OH to give the corresponding alkoxides and the methanol [22–25]. By pumping away the methanol, the resulting alkoxides were isolated as the salts. Then the nucleophilic attack by the moisture-sensitive alkoxides on 4,4′- or 5,5′-bis($BrCH_2$)-2,2′-bpy [40] in the dry solvent (e.g. THF) gave rise to the synthesis of 4,4′- or 5,5′-substituted bpy ligands, [bis($R_fCH_2OCH_2$)-2,2′-bpy)] (**1a**–**d**, **2a**–**d**; Scheme 1; the mass spectral studies of these ligands are shown as supplementary information). The Pd complexes with the fluorous chain at the 4,4′- or 5,5′-positions, **3a**–**c** and **4a**–**b**, were then easily synthesized by stirring the respective ligand and metal precursor, [$PdCl_2(CH_3CN)_2$], at room temperature overnight. Accordingly, the Pt complexes with the fluorous chain, **5a**–**b** (at 4,4′-positions) and **6a** (at 5,5′-positions) were also prepared by stirring the respective ligand and platinum halides overnight (Scheme 1). Single crystals of four metal complexes (**3a**–**6a**) were grown by diffusion crystallization.

2.2. Molecular structures

Although previously reported X-ray structures of Pd and Pt complexes carrying fluorous segments were primarily phosphine-ligand based [30–33], reported herein are the complex structures of **3a**–**6a** that contain the less common poly-fluorinated 2,2′-bpy ligands [26,28,34–38]. Four single crystal structures were obtained among these new poly-fluorinated compounds. They are the two Pd complexes **3a** and **4a** and the two Pt complexes **5a** and **6a**. Their structures are elucidated and discussed below. Because **3a** and **5a** are isostructural to each other, and the structures of **4a** and **6a** are very similar, we will discuss the structural features of **3a** and **5a** together as a pair. Likewise, the structures of **4a** and **6a** will be discussed together.

2.2.1. Structures of Pd and Pt complexes 3a and 5a (both 3a and 5a are isostructural to each other)

The molecular structure of Pd complex **3a** was collected with $R = 0.0286$ being in the $P2_1/c$ space group. In the case of **3a** as shown in Fig. 3, one molecule exists in the asymmetric unit in which the molecular plot of **3a** has one disordered CF_3 group and one non-disordered CF_3 group. Compound **3a** crystallizes with a slightly distorted square-planar geometry. The molecule may have an approximate two-fold symmetry. The Pd(1)–N(1) and Pd(1)–Cl(1) distances are within the expected ranges at 2.021(2) and 2.292(1) Å, respectively. The other selected bond lengths and bond angles in the first metal sphere are normal and also listed in Fig. 2. The π–π interaction is clearly seen in the crystal structures of **3a**, and the distance between two stacking bpy planes is 3.402 Å. This π–π interaction is believed to be the primary driving force in crystallization for this type of complex. As shown in Fig. 2, the structure of **3a** also has a noted feature on the ethereal O-linker [10], which conforms to an intramolecular 5-membered C–H…O hydrogen bonded system. From its schematic drawing in Fig. 3(I), the special intramolecular 5-membered hydrogen bonded system is easily formed by each oxygen atom with its neighboring H3′ or H3 atom.

The special features of **3a** are its unique $–CH_2OCH_2CF_3$ chain at the 4 (4′) position and the formation of intramolecular 5-membered C–H…O hydrogen bond, etc. Compound **3a** is obviously the simplest analogue among these Group 10 metal complexes [24], [MCl_2(4,4′-bis($R_fCH_2OCH_2$)-2,2′-bpy)], where $R_f = CF_3$ (**3a**), C_3F_7 (**3c**), M = Pd; $R_f = C_3F_7$ (**5c**), M = Pt. Also shown in Fig. 3(I), the 5-membered region from **3a** demonstrates an unusual structural parameters of C–H…O H-bonding, i.e., the torsion angles (C3–C4–C–O, C3′–C4′–C–O) are relatively small being −16.97° and 3.97°; distances (O…H3, O′…H3′) is 2.449 and 2.503 Å are shorter than the sum, 2.77 Å [41], of van der Waals radii of H and O atoms, and bond angles (C3–H1…O, C3′–H1′…O′) are close to 100° (100.90° and 100.08°). When comparing these data with the relevant structural parameters from its analogues, **3c** and **5c** [24], the results suggest that a similar 5-membered C–H…O H-bonding, as shown in Fig. 3(III), can readily be formed as the bpy–CH_2–O ethereal linkage can easily rotate along the C(ring)–C(benzylic) bond and bend toward the H3 (H3′) and H5 (H5′) atoms situated nearby.

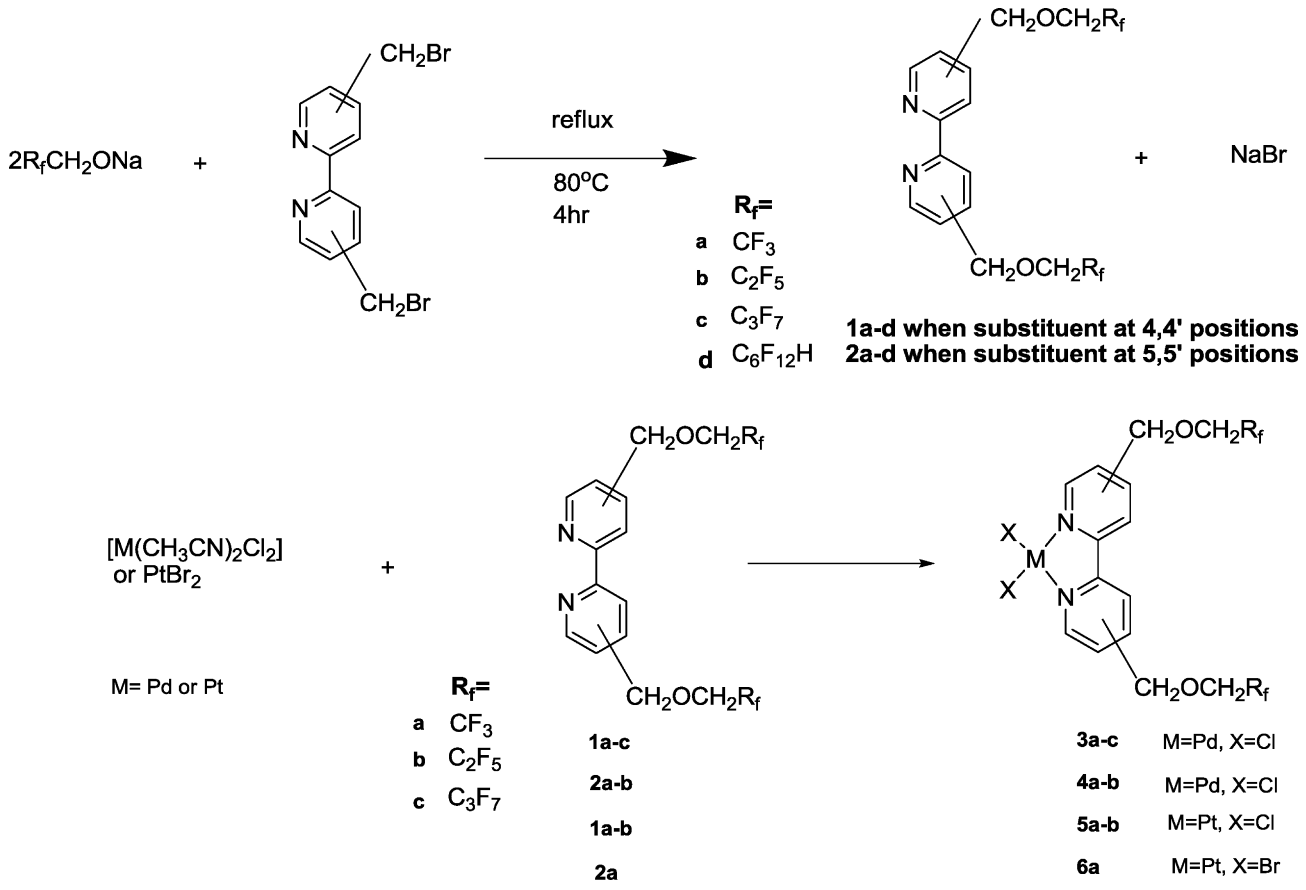

Scheme 1. Synthesis of **1a–d**, **2a–d**, **3a–c**, **4a–b**, **5a–b** and **6a**.

The intramolecular five-membered C–H. . .O hydrogen bonding system of **3a** and **3c** is schematically shown in Fig. 3(I) and (III), respectively. Thus, due to the less hindered CF_3 group, the O atom from **3a** intramolecularly forms 5-membered hydrogen bonding with the H3 atom. In contrast, O atom from complex **3c** which has longer group, C_3F_7, forms the intramolecular 5-membered hydrogen bonding with the H5 atom instead to avoid the steric hindrance

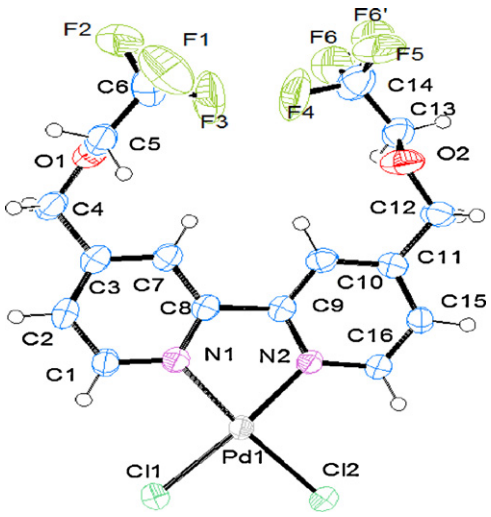

Fig. 2. The ORTEP view of **3a**. (Displacement ellipsoids are drawn at the 25% probability level.) Selected bond lengths (Å) and bond angles (°): Pd(1)–N(1) 2.021(2), Pd(1)–N(2) 2.024(2), Pd(1)–Cl(1) 2.292(1), Pd(1)–Cl(2) 2.294(1); N(1)–Pd(1)–N(2) 80.4(1), Cl(1)–Pd(1)–Cl(2) 90.7(0), N(1)–Pd(1)–Cl(1) 94.2(0), N(1)–Pd(1)–Cl(2) 80.4(1), N(2)–Pd(1)–Cl(1) 174.7(0), N(2)–Pd(1)–Cl(2) 94.7(0).

from two $-CH_2OCH_2R_f$ groups. Furthermore, it is easy to see that the selected bond lengths and bond angles around the metal center from metal complexes of this type are normal. That is to say the geometric influence of $R_fCH_2OCH_2-$ ponytail on the first metal sphere is minimal. This $R_fCH_2OCH_2-$ ponytail is found to form the several weak H-bonding interactions via the interaction of very electronegative F or O atom with the acidic methylene hydrogen atoms.

However, as shown in Fig. 3(II), complex **4a** (or **6a**) with the fluorous substituents at the 5,5′-positions has a totally different orientation of the fluorous ponytails from those of **3a** (or **5a**). The intramolecular five-membered C–H. . .O hydrogen bonding system is missing in **4a** (or **6a**), and the O atoms are located in a way that the O-containing side arms are almost perpendicular to the molecular plane of metal complex. In order to offset this destabilizing orientation where no 5-membered ring is formed, two of aromatic H atoms form H-bonding with two halides from adjacent metal complexes. These will be discussed again in the case of **6a** (or **4a**) below.

As for the **5a**, its structure is exactly analogous to that of **3a**. As shown in Fig. 4, the π–π stacking of 3.519 Å interaction is also the primary driving force for crystallization for this type of complex. Its selected bond lengths (Å) and bond angles (°) are given in Fig. 4.

2.2.2. Structures of complexes 4a and 6a

Complex **4a** was prepared by simply reacting ligand **2a** with the Pd precursor, $[PdCl_2(CH_3CN)_2]$. The ORTEP diagram of structure **4a** is shown in Fig. 5, and its selected bond lengths and bond angles in the first metal sphere are normal and are also listed there.

However, complex **4a** (or **6a**) prepared by using the 5,5′-substituted ligand **2a** as a chelating reagent shows very different structural features from those of **3a** and **5a** with respect to the

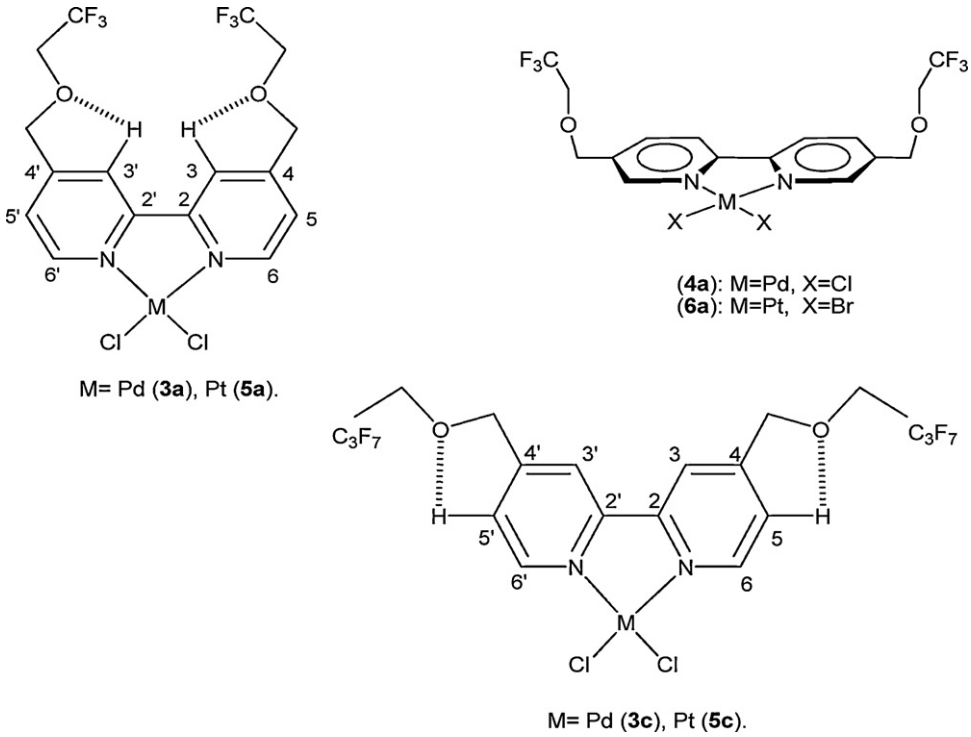

Fig. 3. (I: upper left) the molecular structure of complex **3a** forming 5-membered O. . .H–C H-bonding with the H atom at 3 (or 3′) position; (II; upper right) the O atoms are located in a way that the O-containing side arm is almost perpendicular to the molecular plane of metal complex; (III; bottom) due to the bulky R_f-containing ponytails, the O atom from the structure at the bottom forms the 5-membered O. . .H–C H-bonding with the H atom at 5 (or 5′) position instead (M = Pd or Pt).

orientation of the ponytails in their structures, as demonstrated previously in Fig. 3. The schematic drawing of the head-to-tail hydrogen bonding of complex **4a** is shown in Fig. 6. As stated earlier, the ponytails of **4a**, unlike **3a** and **5a**, were orthogonal to the core metal plane, so the O atom of a fluorous ponytail from **4a** cannot form the five-membered ring with any bipyridyl hydrogen located in the orthogonal plane. In other words, the weak intramolecular C–H. . .O interaction that was easily observed in **3a** (or **5a**), which has the substituents at the 4,4′ positions, was missing in the case of **4a** (or **6a**). However, some other favorable weak interactions that include 1-D head-to-tail interactions, as shown in Fig. 6, have been formed to link the molecules together to compensate the aforementioned destabilizing forces.

In addition, the intermolecular structure of **4a** is also interesting. These fluorous chain interactions seem to help the stacking of two adjacent square planar Pd complexes. As shown in Fig. 7, alternating distances of 3.457 Å and 4.004 Å exist among the layers of square planar Pd complexes. The distance of 3.457 Å is the shorter distance between the Pd dimer, which seems to show the Pd and Pd metal interaction, and this interaction results from the fluorous chain interactions within this dimer. In contrast, and the other spacing between the other two monomers (or dimer) is 4.004 Å, which is certainly longer than 3.457 Å, and it is easy to see that no fluorous side chain interactions exist within this distance. Therefore, these two different distances are simply the results of whether or not the fluorous side chain interaction is present within the dimers. The

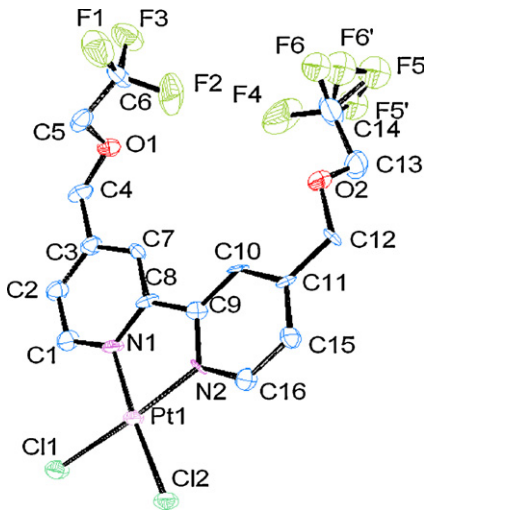

Fig. 4. The ORTEP view of **5a**. (Displacement ellipsoids are drawn at the 25% probability level.) Selected bond lengths (Å) and bond angles (°): Pt(1)–N(1) 2.000(11), Pt(1)–N(2) 1.987(10), Pt(1)–Cl(1) 2.303(4), Pt(1)–Cl(2) 2.300(4); N(1)–Pt(1)–N(2) 81.3(5), Cl(1)–Pt(1)–Cl(2) 90.1(1), N(1)–Pt(1)–Cl(1) 94.3(4), N(1)–Pt(1)–Cl(2) 175.6(4), N(2)–Pt(1)–Cl(1) 175.6(3), N(2)–Pt(1)–Cl(2) 94.3(3).

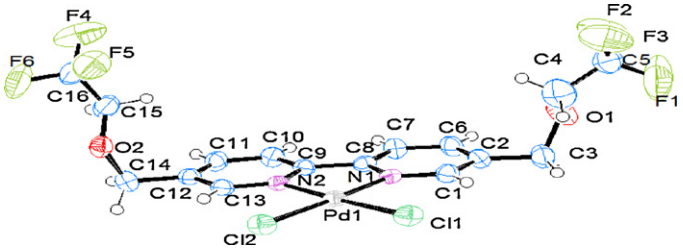

Fig. 5. The ORTEP view of **4a**. Selected bond lengths (Å) and bond angles (°): Pd(1)–N(1) 2.036(4), Pd(1)–N(2) 2.032(4), Pd(1)–Cl(1) 2.293(1), Pd(1)–Cl(2) 2.295(1); N(1)–Pd(1)–Cl(1) 94.4(1), N(1)–Pd(1)–Cl(2) 174.9(1), N(2)–Pd(1)–Cl(1) 175.2(1), N(2)–Pd(1)–Cl(2) 94.1(1), Cl(1)–Pd(1)–Cl(2) 90.7 (0).

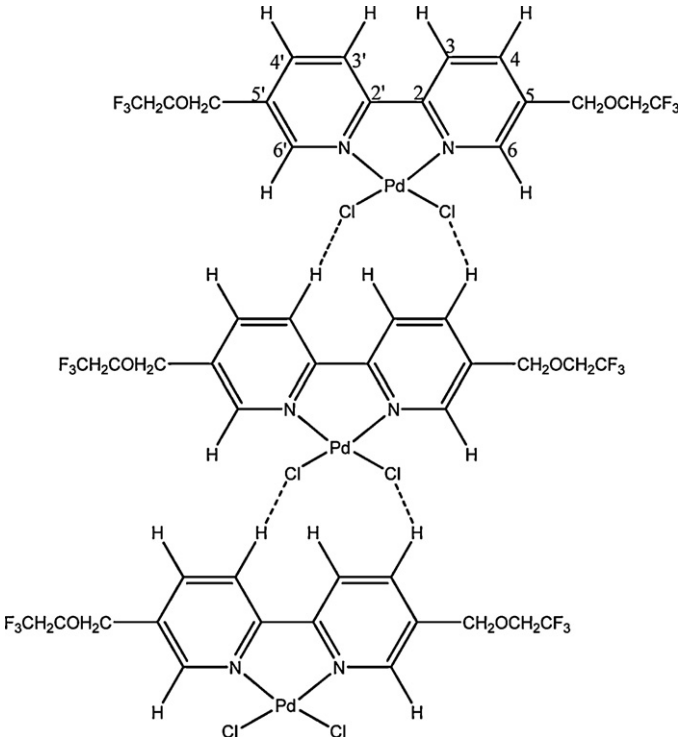

Fig. 6. The head-to-tail H-bonding interaction between two Cl atoms and two aromatic H atoms (H3′ and H4) from the Pd complex **4a**.

inter-monomer distance of 3.457 Å, which is formed by the fluorous chain interactions, is clearly shorter than the distance, 4.004 Å, to the next pair.

2.2.3. Structure of Pt complex 6a

As for the structure of **6a**, whose structural features are similar to those of **4a**, it is more symmetric in the sense of its more ordered intermolecular interactions. For example, two Br atoms symmetrically form H-bonding with the 3,3′-hydrogens from the immediately neighboring molecule in **6a**. In contrast, in the case of **4a**, its two Cl atoms form the H-bonding with the H atoms situated at the 3′ and 4 aromatic positions instead (Fig. 6).

As shown in Fig. 8, an 8-membered cavity is formed by a pair of rare C–H...F–C and C–F...H–C weak interactions. To the best of our knowledge, this type of 8-membered cavity has never been reported before. Furthermore, the 8-membered cavities formed from these two columnar chains are actually in the different layers. The left 1-D chain is situated one layer above 1-D chain on the right because of the crystal slippage. Due to the electron and electron repulsion, the layers immediately above and below the left 1-D chain are anti-parallel to its linking direction (see Figs. 6 and 8). Furthermore, as stated above in the case of **4a**, two extended molecular chains of **6a** in the b-related direction are linked together due to the weak intermolecular interactions between each Br atom and its corresponding aromatic H atom (H3 or H3′) of an adjacent molecule.

As shown in Fig. 9, the structure of complex **6a**, which also has two different spacings like those described above (in **4a** case), is similar to the recently reported structure of [$PtBr_2$bpy] [42,43]. This structure is also different from either the red or yellow form of [$PtCl_2$bpy] [44,45]. The two nonequivalent Pt–Br bonds are 2.420(1) and 2.426(1) Å, respectively. Accordingly, the two nonequivalent Pt–N bonds are 2.026(4) and 2.022(5) Å, which are obviously longer than 2.000(11) and 1.987(10) Å of two nonequivalent Pt–N bonds from **5a** due to the larger trans effect of a Br atom in **6a** over a Cl atom in **5a**. In particular, two different Pt–Pt interactions observed are 3.504 and 4.762 Å for the spacing within the fluorous chain inter-connected dimer, and for the other spacing between the two discrete monomers without the fluorous side chain interactions in between, respectively. Thus, although the chain-like structure of Pt...Pt...Pt orientations were observed in the case of **6a**, only the short Pt...Pt distance of 3.504 Å shows the possibility of weak Pt–Pt bonding, while the other long Pt...Pt distance of 4.762 Å is obviously too long to have any substantial metal to metal interaction. As stated above, the fluorous side chains are certainly helpful in binding two monomers together to form a dimer with the shorter spacing of 3.504 Å.

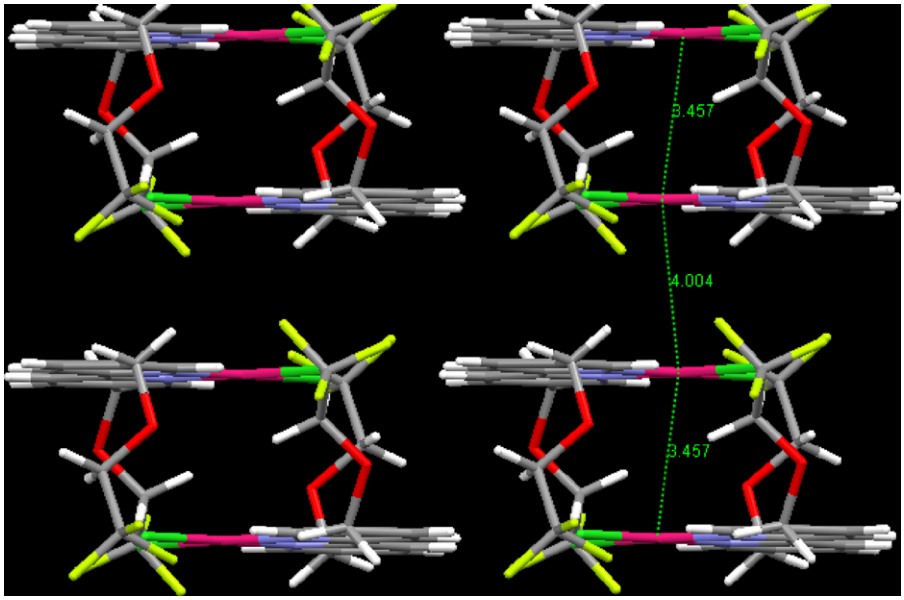

Fig. 7. The side view of structure of complex **4a** (H, white; C, carbon; O, red; N, blue; Cl, green; F, yellow; Pd, pink). (For interpretation of the references to color in this figure legend, the reader is referred to the web version of the article.)

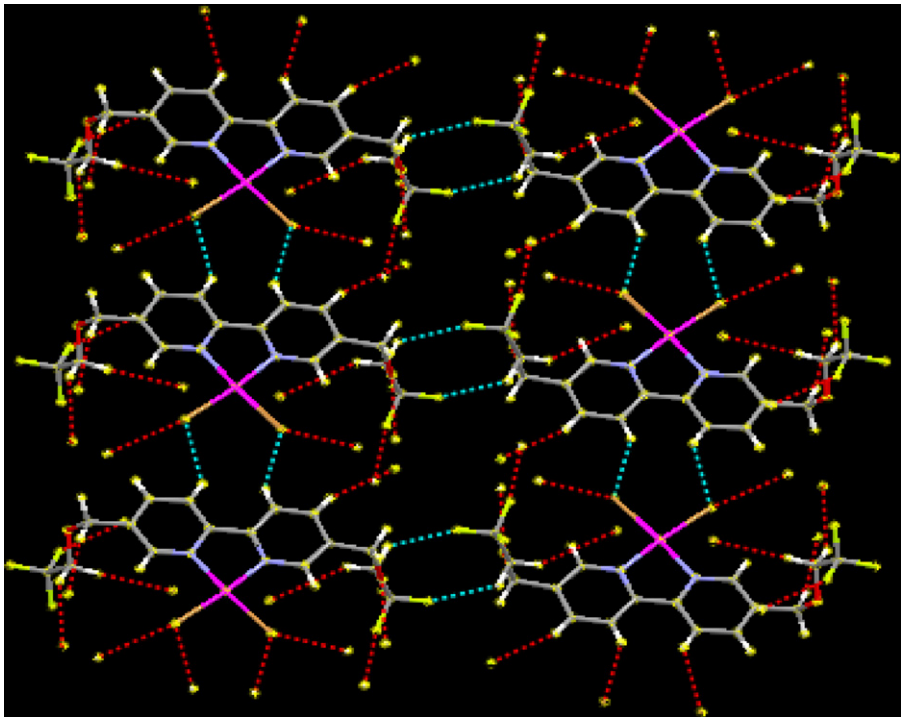

Fig. 8. The unique 8-membered synthon connected two adjacent stacks together. The head to tail link between the two neighboring molecules (H, white; C, carbon; O, red; N, blue; F, yellow; Br, brown; Pt, purple). (For interpretation of the references to color in this figure legend, the reader is referred to the web version of the article.)

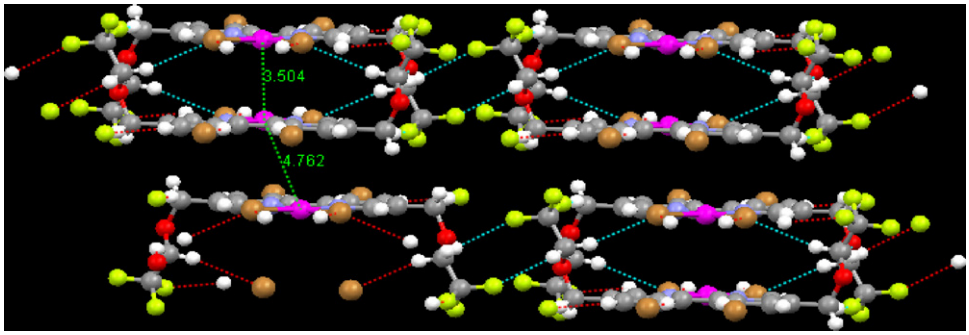

Fig. 9. The interconnected dimer with the shorter Pt...Pt distance of 3.504 Å was brought together by the interactions between fluorous side chains. In addition, two adjacent columnar structures were linked together by the unique 8-membered cavity which is formed by a pair of rare C–H...F–C and C–F...H–C weak interactions.

3. Conclusions

In this article we report the successful synthesis of two series of fluorous ligands (**1a**–**d**, **2a**–**d**) and some of their Pd or Pt complexes. Additionally, X-ray structures of single crystals of four metal complexes, **3a**–**6a**, were determined. As a summary on the X-ray structural features, first, the π–π stacking of bpy skeletons are commonly observed for all four complexes. Secondly, the intramolecular five-membered C–H...O weak hydrogen bonding interactions to extend the fluorous ponytail in a fixed orientation were observed for **3a** and **5a**, but were missing for **4a** and **6a** whose ligands have the substitutents at the 5,5′ positions instead. In the case of **6a**, a unique 8-membered cavity was formed by a pair of rare C–H...F–C and C–F...H–C weak interactions, which as far as we know has never been reported. Due to the unusual structural features from the fluorous chain interactions of both **4a** and **6a**, their photophysical properties might be interesting and will be investigated in the near future.

4. Experimental

4.1. General

The gas chromatographic/mass spectrometric (GC/MS) data were taken using an Agilent 6890 Series gas chromatograph with a series 5973 mass selective detector. The GC monitoring employed a HP 6890 GC using a 30 m × 0.250 mm HP-5 capillary column with a 0.25 μm stationary phase film thickness. Both electron impact (EI) and chemical ionization (CI) modes are used to study the fluorous ligands. Methane is used as a carrier gas in the CI mode. Infrared spectra were obtained on a Perkin Elmer RX I FT-IR Spectrometer. NMR spectra were recorded on a Bruker AM 500 MHz instrument using 5 mm sample tubes. The residual peaks of CD_3OD, CD_2Cl_2, $CDCl_3$, deuterated Me_2SO and deuterated DMF were used as the reference peaks for both ^1H and ^{13}C NMR spectra; that of Freon® 11 ($CFCl_3$) for ^{19}F NMR spectra. Fast atom bombardment (FAB) mass spectrometry analysis was

provided by the staff of the National Central University (Taiwan) Mass Spectrometry Laboratory.

4.2. Starting materials

Chemicals, reagents, and solvents employed were commercially available and used as received. The CF_3CH_2OH, $C_2F_5CH_2OH$, $C_3F_7CH_2OH$, and $HCF_2(CF_2)_5CH_2OH$ were purchased from Sigma–Aldrich or SynQuest Laboratories.

4.3. Preparation of 4,4′- and 5,5′-bis($R_fCH_2OCH_2$)-2,2′-bpy, [R_f = CF_3 (**a**), C_2F_5 (**b**), n-C_3F_7 (**c**), $HCF_2(CF_2)_5$ (**d**); see Fig. 1 for the numbering]

General procedure: The 30% CH_3ONa/CH_3OH (1.1 g) and R_fCH_2OH (6.0 mmol) were charged into a round-bottomed flask, then continuously stirred at ca 80 °C under N_2 atmosphere for 4 h before CH_3OH was vacuum removed. The resulting fluorinated alkoxide (6.0 mmol) was then dissolved in 20 mL of dry THF, and bis($BrCH_2$)-2,2′-bpy (5.8 mmol; at 4,4′- or 5,5′-positions) added. The mixture was brought to reflux for overnight, and the completeness of the reaction was checked by the GC/MS. After the reaction, the solvent was removed by vacuum pump. The crude product was extracted using the separatory funnel from the CH_2Cl_2/H_2O system several times. Then the crude product was further purified by either vacuum sublimation or column chromatography to obtain white solids.

4.4. Preparation of 4,4′-bis($R_fCH_2OCH_2$)-2,2′-bpy, [where R_f = CF_3 (**1a**), C_2F_5 (**1b**), n-C_3F_7 (**1c**), $HCF_2(CF_2)_5$ (**1d**)]; {some analytical data of **1a** and **1c** were reported in Refs. [22,24], respectively. The more complete data of these two ligands are listed below}

The specific ligand was usually purified by vacuum sublimation to obtain white solids. The vacuum level was 0.1 Torr, and the sublimation temperature was normally 50 °C above its mp.

Analytical data of **1a**: Yield 86%, m.p. = 83 °C (500 MHz, d-DMSO): δ = 8.68 (2H, d, $^3J_{H-H}$ = 5.0 Hz, H-6), 8.38 (2H, s, H-3), 7.41 (2H, d, $^3J_{H-H}$ = 5.0 Hz, H-5), 4.83 (4H, s, bpy–C**H**$_2$), 4.22 (4H, q, $^3J_{H-F}$ = 9.2 Hz, C**H**$_2$CF$_3$). ^{19}F NMR (470.5 MHz, d-DMSO): δ = −73.2 (6F, t, $^3J_{H-F}$ = 8.6 Hz, CH_2C**F**$_3$). ^{13}C NMR (126 MHz, d-DMSO), δ = 155, 149, 148, 122, 118 (10C, s, bpy), 125 (128–121, q, $^1J_{C-F}$ = 280.4 Hz, **C**F$_3$), 72 (2C, s, bpy–**C**H$_2$), 67 (2C, q, –**C**H_2CF_3, $^2J_{C-F}$ = 32.3, **C**). FT-IR (KBr; cm^{-1}): 1603, 1560, 1440 (bpy-ring, m) 1178, 1153 (CF_2 stretch, s).

GC/MS (*m*/*z*; EI mode): 380.1 $[M]^+$, 281.0 $[M-C_2H_3F_3O]^+$, 182.1 $[M-(C_2H_3F_3O)_2]^+$, 91 $[M-(C_2H_3F_3O)_2C_6H_5N]^+$.

(*m*/*z*; CI mode): 420.9 $[M+C_3H_5]^+$, 408.9 $[M+C_2H_5]^+$, 380.9 $[M+H]^+$, 360.9 $[M-HF]^+$, 340.9 $[M-(HF)_2]^+$, 280.9 $[M-OCH_2CF_3]^+$, 182.9 $[M-(OCH_2CF_3)_2+H]^+$, 100.9 $[OCH_3CF_3+H]^+$, 80.9 $[OCH_3CF_3-HF+H]^+$.

Analytical data of **1b**: Yield 71%; ^{1}H NMR (500 MHz, *d*-Me_2SO): δ = 8.68 (2H, d, $^3J_{H-H}$ = 5.1 Hz, H-6), 8.37 (2H, s, H-3), 7.39 (2H, d, $^3J_{H-H}$ = 5.1 Hz, H-5), 4.84 (4H, s, bpy–C**H**$_2$), 4.30 (4H, t, $^3J_{H-F}$ = 14.0 Hz, CF_2C**H**$_2$). ^{19}F NMR (470.5 MHz, *d*-Me_2SO): δ = −83.0 (6F, CF_2C**F**$_3$), −122.9 (4F, t, $^3J_{H-F}$ = 13.5 Hz, CH_2C**F**$_2$); ^{13}C NMR (126 MHz, *d*-Me_2SO): δ = 72 (bpy–**C**H_2), 66 (bpy–CH_2O**C**H_2), 111–122 (**C**$_2$F$_5$), 118, 122, 147, 150, 155 (bpy); FT-IR (KBr; cm^{-1}): 1601m, 1561m, 1463m (*ν*bpy), 1196vs, 1132vs (*ν*CF_2); m.p. = 40 °C.

GC/MS (*m*/*z*; EI mode): 480.1 $[M]^+$, 332.1 $[M-OCH_2C_2F_5+H]^+$, 198.1 $[M-O(CH_2C_2F_5)_2]^+$, 183.1 $[M-(OCH_2C_2F_5)_2+H]^+$, 91.1 $[M-(OCH_2C_2F_5)_2-C_6H_5N]^+$.

(*m*/*z*; CI mode): 520.9 $[M+C_3H_5]^+$, 508.9 $[M+C_2H_5]^+$, 480.9 $[M+H]^+$, 330.9 $[M-OCH_2C_2F_5]^+$, 182.9 $[M-(OCH_2C_2F_5)_2+H]^+$, 150.9 $[OCH_3C_2F_5+H]^+$, 130.9 $[OCH_3C_2F_5-HF+H]^+$.

Analytical data of **1c**: Yield 86.2%; ^{1}H NMR (500 MHz, d-Me_2SO) δ_H 8.67 (2H, d, $^3J_{H-H}$ = 4.5 Hz, 2× H_6), 8.37 (2H, s, 2× H_3), 7.38 (2H, d, $^3J_{H-H}$ = 4.5 Hz, 2× H_5), 4.84 (4H, s, 2× bpy–C$\underline{H}_2$), 4.34 (4H, t, $^3J_{H-F}$ = 14.5 Hz, 2× $CF_2C\underline{H}_2$); ^{19}F NMR (470.5 MHz, d-Me_2SO) δ_F −80.4 (t, $^3J_{H-F}$ = 9 Hz, CF_3), −119.7 (m, $CF_3C\underline{F}_2CF_2$), −126.8 (s, $CF_3CF_2C\underline{F}_2$); ^{13}C NMR (113 MHz, d-Me_2SO) δ_C 72 (bpy–*C*H_2), 67 (*C*H_2CF_2), 119, 122, 148, 150, 155 (bpy), 113–117 (*C*$F_2CF_2CF_3$); FT-IR (KBr; cm^{-1}): 1596m, 1558m (*ν*bpy), 1225vs, 1120vs (*ν*CF_2); m.p. = 68–70 °C.

GC/MS (EI): 580 (M^+), 382 ($M^+-OCHC_3F_7$), 183 ($C_5H_3NCH_2C_5H_3NCH_3^+$), 91 ($C_5H_3NCH_2^+$).

(*m*/*z*; CI mode): 620.9 (M^++C_3H_5), 608.9 (M^++C_2H_5), 580.9 (M^++H), 380.9 ($M^+-OCH_2C_3F_7$), 182.9 ($M^+-(OCH_2C_3F_7)_2$+H), 200.8 ($OCH_3C_3F_7$+H), 180.8 ($OCH_3C_3F_7$−HF+H).

(*m*/*z*; CI mode): 620.9 $[M+C_3H_5]^+$, 608.9 $[M+C_2H_5]^+$, 580.9 $[M+H]^+$, 380.9 $[M-OCH_2C_3F_7]^+$, 182.9 $[M-(OCH_2C_3F_7)_2+H]^+$, 200.8 $[OCH_3C_3F_7+H]^+$, 180.8 $[OCH_3C_3F_7-HF+H]^+$.

Analytical data of **1d**: Yield 74%; ^{1}H NMR (500 MHz, *d*-Me_2SO): δ = 8.66 (2H, d, $^3J_{H-H}$ = 4.94 Hz, H-6), 8.36 (2H, s, H-3), 7.38 (2H, d, $^3J_{H-H}$ = 5.00 Hz, H-5), 7.16 (2H, tt, $^2J_{H-F}$ = 50.3 Hz, $^3J_{H-F}$ = 5.2 Hz, CF_2**H**), 4.77 (4H, s, bpy–C**H**$_2$), 4.17 (4H, t, $^3J_{H-F}$ = 14.6 Hz, CF_2C**H**$_2$). ^{19}F NMR (470.5 MHz, *d*-Me_2SO): δ = −118.7, −122.1, −122.9, −123.1, −129.0 (20F; CH_2(C**F**$_2$)$_5$), −138.4 (4F, d, $^2J_{H-F}$ = 50.5 Hz, HC**F**$_2$). ^{13}C NMR (126 MHz, *d*-Me_2SO): δ = 72 (bpy–**C**H_2), 67 (bpy–CH_2O**C**H_2), 106–116 (**C**$_6$F$_{12}$), 118, 122, 147, 149, 155 (bpy); FT-IR (KBr; cm^{-1}): 1598, 1561, 1465 (m, *ν*bpy), 1196, 1137 cm^{-1} (vs, *ν*CF_2); m.p. = 68 °C.

GC/MS (*m*/*z*; EI mode): 844.1 $[M]^+$, 514.1 $[M-OCH_2C_6F_{12}H+H]^+$, 198.1 $[M-O(CH_2C_6F_{12}H)_2]^+$, 183.1 $[M-(OCH_2C_6F_{12}H)_2+H]^+$, 91.1 $[M-(OCH_2C_6F_{12}H)_2-C_6H_5N]^+$.

(*m*/*z*; CI mode): 884.9 $[M+C_3H_5]^+$, 872.9 $[M+C_2H_5]^+$, 844.9 $[M+H]^+$, 512.8 $[M-OCH_2C_6F_{12}H]^+$, 182.9 $[M-(OCH_2C_6F_{12}H)_2+H]^+$, 332.8 $[OCH_3C_6F_{12}H+H]^+$, 312.8 $[OCH_3C_6F_{12}H-HF+H]^+$.

4.5. Preparation of 5,5′-bis($R_fCH_2OCH_2$)-2,2′-bpy, [R_f = CF_3 (**2a**), C_2F_5 (**2b**), n-C_3F_7 (**2c**), $HCF_2(CF_2)_5$ (**2d**)]

The ligand was usually purified by vacuum sublimation to obtain white solids. The vacuum level was 0.1 Torr, and the sublimation temperature was normally 50 °C above its m.p.

Analytical data of **2a**: Yield 75%; ^{1}H NMR (500 MHz, *d*-Me_2SO): δ = 8.66 (2H, s, H-6), 8.39 (2H, d, $^3J_{H-H}$ = 8.24 Hz, H-4), 7.92 (2H, d, $^3J_{H-H}$ = 8.24 Hz, H-3), 4.77 (4H, s, bpy–C**H**$_2$), 4.17 (4H, q, $^3J_{H-F}$ = 9.34 Hz, CF_3C**H**$_2$). ^{19}F NMR (470.5 MHz, *d*-Me_2SO): δ = −73.1 (6F, t, $^3J_{H-F}$ = 10.8 Hz, CH_2C**F**$_3$). ^{13}C NMR (126 MHz, *d*-Me_2SO): δ = 71 (bpy–**C**H_2), 67 (bpy–CH_2O**C**H_2), 121–128 (**C**F$_3$), 120, 133, 137, 149, 155 (bpy); FT-IR [ν_{max}(KBr)/cm^{-1}]: 1598m, 1554m, 1469m, 1359m (*ν*bpy), 1156vs, 1123vs (*ν*CF_2); m.p. = 120 °C.

GC/MS (*m*/*z*; EI mode): 380.1 $[M]^+$, 297.1 $[M-CH_2CF_3]^+$, 281.1 $[M-OCH_2CF_3]^+$, 198.1 $[M-O(CH_2CF_3)_2]^+$, 182.1 $[M-(OCH_2CF_3)_2]^+$, 91.1 $[M-(OCH_2CF_3)_2-C_6H_5N]^+$.

(*m*/*z*; CI mode): 420.9 $[M+C_3H_5]^+$, 408.9 $[M+C_2H_5]^+$, 381 $[M+H]^+$, 360.9 $[M-HF]^+$, 340.9 $[M-(HF)_2]^+$, 281 $[M-OCH_2CF_3]^+$, 198.9 $[M-O(CH_2CF_3)_2+H]^+$, 100.9 $[OCH_3CF_3+H]^+$, 80.9 $[OCH_3CF_3-HF+H]^+$.

Note: The structure of **2a** was reported in the crystallographic journal [39], but its detailed preparation and completely characterized data are only given here.

Analytical data of **2b**: Yield 76%; ^{1}H NMR (500 MHz, *d*-Me_2SO): δ = 8.64 (2H, s, H-6), 8.39 (2H, d, $^3J_{H-H}$ = 8.51 Hz, H-4), 7.89 (2H, d, $^3J_{H-H}$ = 8.24 Hz, H-3), 4.77 (4H, s, bpy–C**H**$_2$), 4.23 (4H, t, $^3J_{H-F}$ = 14.01 Hz, CF_3C**H**$_2$). ^{19}F NMR (470.5 MHz, *d*-Me_2SO): δ = −122.9 (4F, t, $^3J_{H-F}$ = 15.0 Hz, CH_2C**F**$_2$), −83.2 (6F, CH_2CF_2C**F**$_3$). ^{13}C NMR (126 MHz, *d*-Me_2SO): δ = 71 (bpy–**C**H_2), 66 (bpy–CH_2O**C**H_2), 111–122 (**C**$_2$F$_5$), 120, 133, 137, 149, 155 (bpy); FT-IR [ν_{max}(KBr)/cm^{-1}]: 1602m, 1554m, 1469m, 1366m (*ν*bpy), 1189vs, 1152vs, 1115vs (*ν*CF_2); m.p. = 106 °C.

GC/MS (*m*/*z*; EI mode): 480.1 $[M]^+$, 347.1 $[M-CH_2C_2F_5]^+$, 331.1 $[M-OCH_2C_2F_5]^+$, 198.1 $[M-O(CH_2C_2F_5)_2]^+$, 182.1 $[M-(OCH_2C_2F_5)_2]^+$, 91.1 $[M-(OCH_2C_2F_5)_2-C_6H_5N]^+$.

(*m*/*z*; CI mode): 520.9 $[M+C_3H_5]^+$, 508.9 $[M+C_2H_5]^+$, 480.9 $[M+H]^+$, 330.9 $[M-OCH_2C_2F_5]^+$, 198.9 $[M-O(CH_2C_2F_5)_2+H]^+$, 150.9 $[OCH_3C_2F_5+H]^+$, 130.9 $[OCH_3C_2F_5-HF+H]^+$.

Analytical data of **2c**: Yield 80%; ^{1}H NMR (500 MHz, *d*-Me_2SO): δ = 8.64 (2H, s, H-6), 8.39 (2H, d, $^3J_{H-H}$ = 7.97 Hz, H-4), 7.90 (2H, d, $^3J_{H-H}$ = 8.24 Hz, H-3), 4.78 (4H, s, bpy–C**H**$_2$), 4.28 (4H, t, $^3J_{H-F}$ = 14.28 Hz, $CF_3C\mathbf{H}_2$). ^{19}F NMR (470.5 MHz, *d*-Me_2SO): δ = −127.5 (4F, s, $CH_2C\mathbf{F}_2$), −120 (4F, m, $CH_2CF_2C\mathbf{F}_2$), −80.8 (6F, t, $^3J_{F-F}$ = 8.63 Hz, $CF_2C\mathbf{F}_3$). ^{13}C NMR (126 MHz, *d*-Me_2SO): δ = 71 (bpy–**C**H_2), 66 (bpy–$CH_2O\mathbf{C}H_2$), 105–118 ($\mathbf{C}_3F_7$), 120, 133, 137, 149, 155 (bpy); FT-IR [ν_{max}(KBr)/cm^{-1}]: 1606m, 1554m, 1473m, 1359 (νbpy), 1174vs, 1119 vs (νCF_2).

GC/MS (*m*/*z*; EI): 580 $[M]^+$, 397 $[M-CH_2C_3F_7]^+$, 381 $[M-OCH_2C_3F_7]^+$, 182 $[M-(OCH_2C_3F_7)_2]^+$; m.p. = 95 °C.

GC/MS (*m*/*z*; EI mode): 580.1 $[M]^+$, 397.1 $[M-CH_2C_3F_7]^+$, 381.1 $[M-OCH_2C_3F_7]^+$, 198.1 $[M-O(CH_2C_3F_7)_2]^+$, 182.1 $[M-(OCH_2C_3F_7)_2]^+$, 91.1 $[M-(OCH_2C_3F_7)_2-C_6H_5N]^+$.

(*m*/*z*; CI mode): 620.9 $[M+C_3H_5]^+$, 608.9 $[M+C_2H_5]^+$, 580.9 $[M+H]^+$, 380.9 $[M-OCH_2C_3F_7]^+$, 198.9 $[M-O(CH_2C_3F_7)_2+H]^+$, 200.9 $[OCH_3C_3F_7+H]^+$, 180.9 $[OCH_3C_3F_7-HF+H]^+$.

Analytical data of **2d**: Yield 92%; ^{1}H NMR (500 MHz, *d*-Me_2SO): δ = 8.65 (2H, s, H-6), 8.38 (2H, d, $^3J_{H-H}$ = 8.2 Hz, H-4), 7.90 (2H, d, $^3J_{H-H}$ = 8.2 Hz, H-3), 7.15 (2H, tt, $^2J_{H-F}$ = 50.0 Hz, $^2J_{H-F}$ = 5.2 Hz, $CF_2\mathbf{H}$), 4.78 (4H, s, bpy–C**H**$_2$), 4.27 (4H, t, $^3J_{H-H}$ = 14.6 Hz, $CF_2C\mathbf{H}_2$). ^{19}F NMR (470.5 MHz, d-Me_2SO): δ = −119.2, −122.6, −123.4, −123.5, −129.5 (20F; $CH_2(C\mathbf{F}_2)_5$), −138.8 (4F, d, $^2J_{H-F}$ = 51.6 Hz, $HC\mathbf{F}_2$). ^{13}C NMR (126 MHz, d-Me_2SO): δ = 71 (bpy–**C**H_2), 66 (bpy–$CH_2O\mathbf{C}H_2$), 105–117 ($\mathbf{C}_6F_{12}H$), 120, 133, 137, 149, 155 (bpy); FT-IR [ν_{max}(KBr)/cm^{-1}]: 1602m, 1560m, 1474m (νbpy), 1194vs, 1122vs (νCF_2); m.p. = 96.6 °C.

GC/MS (*m*/*z*; EI mode): 844.1 $[M]^+$, 529.1 $[M-CH_2C_6F_{12}H]^+$, 513.1 $[M-OCH_2C_6F_{12}H]^+$, 198.1 $[M-O(CH_2C_6F_{12}H)_2]^+$, 182.1 $[M-(OCH_2C_6F_{12}H)_2]^+$, 91.1 $[M-(OCH_2C_6F_{12}H)_2-C_6H_5N]^+$.

(*m*/*z*; CI mode): 884.9 $[M+C_3H_5]^+$, 872.9 $[M+C_2H_5]^+$, 844.9 $[M+H]^+$, 512.9 $[M-OCH_2C_6F_{12}H]^+$, 182.9 $[M-(OCH_2C_6F_{12}H)_2+H]^+$, 332.8 $[OCH_3C_6F_{12}H+H]^+$, 312.8 $[OCH_3C_6F_{12}H-HF+H]^+$.

4.6. A single general procedure for preparing all the metal complexes, Pd (3a–b, 4a–b) and Pt (5a–b and 6a) complexes

Equal molar amounts of metal precursor (0.52 mmol) and the specific ligand (0.52 mmol) were charged into a round-bottomed flask, and CH_2Cl_2 (3 mL) was added as solvent. The solution changed color after mixing for several min. The solution was further stirred for 24 h at room temperature before the solvent and volatile materials were removed under vacuum. The resulting colored solid collected this way was spectroscopically pure. Accordingly, the recrystallization proceeded with dissolution of **3a** in DMF to form the saturated solution, to which a methanol overlayer (5 mL) was added. Then, solvent diffusion over a period of a week at 25 °C afforded the specific crystals.

4.7. Preparation of Pd complexes (3a–b), [$PdCl_2$(4,4′-bis($CF_3CH_2OCH_2$)-2,2′-bpy)]

Analytical data of **3a** (from $[PdCl_2(CH_3CN)_2]$ and ligand **1a**): Yield 99%, yellow solid; ^{1}H NMR (500 MHz, *d*-Me_2SO): δ = 9.03 (2H, d, $^3J_{H-H}$ = 6.0 Hz, H-6), 8.43 (2H, s, H-3), 7.73 (2H, d, $^3J_{H-H}$ = 6.0 Hz, H-5), 4.95 (4H, s, bpy–C**H**$_2$), 4.29 (4H, q, $^3J_{H-F}$ = 9.2 Hz, $CF_3C\mathbf{H}_2$). ^{19}F NMR (470.5 MHz, *d*-Me_2SO): δ = −73.1 (6F, t, $^3J_{H-F}$ = 10.8 Hz, $CH_2C\mathbf{F}_3$). ^{13}C NMR (126 MHz, *d*-Me_2SO): δ = 71 (bpy–**C**H_2), 67 (bpy–$CH_2O\mathbf{C}H_2$), 121–128 ($\mathbf{C}F_3$), 156, 152, 150, 125, 121 (bpy); FT-IR [ν_{max}(KBr)/cm^{-1}]: 1619m, 1560m, 1431m (νbpy), 1170vs, 1155vs (νCF_2). HR-MS (FAB): $[M]^+$ $C_{16}H_{14}F_6N_2O_2Pd^{35}Cl_2$ calc. *m*/*z* 555.9367, found 555.9371; $C_{16}H_{14}F_6N_2O_2Pd^{35}Cl^{37}Cl$ calc. *m*/*z* 557.9340, found 557.9342; $C_{16}H_{14}F_6N_2O_2Pd^{37}Cl_2$ calc. *m*/*z* 559.9326, found 559.9312; m.p. = 249 °C.

Analytical data of **3b** (from $[PdCl_2(CH_3CN)_2]$ and ligand **1b**): Yield 96%, yellow solid; ^{1}H NMR (500 MHz, *d*-Me_2SO): δ = 9.02 (2H, d, $^3J_{H-H}$ = 6.0 Hz, H-6), 8.37 (2H, s, H-3), 7.71 (2H, d, $^3J_{H-H}$ = 6.0 Hz, H-5), 4.96 (4H, s, bpy–C**H**$_2$), 4.39 (4H, t, $^3J_{H-F}$ = 14.01 Hz, $CF_3C\mathbf{H}_2$). ^{19}F NMR (470.5 MHz, *d*-Me_2SO): δ = −123.1 (4F, t, $^3J_{H-F}$ = 12.9 Hz, $CH_2C\mathbf{F}_2$), −83.1 (6F, $CF_2C\mathbf{F}_3$). ^{13}C NMR (126 MHz, *d*-Me_2SO): δ = 71 (bpy–**C**H_2), 66 (bpy–$CH_2O\mathbf{C}H_2$), 111–122 ($\mathbf{C}_2F_5$), 156, 152, 150, 125, 121 (bpy); FT-IR [ν_{max}(KBr)/cm^{-1}]: 1622, 1559, 1462, (m, νbpy), 1196, 1158 cm^{-1} (vs, νCF_2). HR-MS (FAB): $[M-Cl]^+$ $C_{18}H_{14}F_{10}N_2O_2Pd^{35}Cl$, calc. *m*/*z* 620.9619, found *m*/*z* 620.9439. $C_{18}H_{14}F_{10}N_2O_2Pd^{37}Cl$, calc. *m*/*z* 622.9589, found *m*/*z* 622.9465; m.p. = 265 °C.

4.8. Preparation of Pd complexes (4a–b), [$PdCl_2$(5,5′-bis($CF_3CH_2OCH_2$)-2,2′-bpy)] (4a–b)

Analytical data of **4a** (from $[PdCl_2(CH_3CN)_2]$ and ligand **2a**): Yield 95%, yellow solid; ^{1}H NMR (500 MHz, *d*-Me_2SO): δ = 9.08 (2H, s, H-6), 8.54 (2H, d, $^3J_{H-H}$ = 8.25 Hz, H-4), 8.28 (2H, d, $^3J_{H-H}$ = 8.24 Hz, H-3), 4.88 (4H, s, bpy_C**H**$_2$), 4.24 (4H, q, $^3J_{H-F}$ = 9.17 Hz, $CF_3C\mathbf{H}_2$). ^{19}F NMR (470.5 MHz, *d*-Me_2SO): δ = −73.1 (6F, t, $^3J_{H-F}$ = 8.62 Hz, $CH_2C\mathbf{F}_3$). ^{13}C NMR (126 MHz, *d*-Me_2SO): δ = 70 (bpy–**C**H_2), 67 (bpy–$CH_2O\mathbf{C}H_2$), 121–128 ($\mathbf{C}F_3$), 123, 137, 140, 148, 156 (bpy). FT-IR [ν_{max}(KBr)/cm^{-1}]: 1617m, 1458m (νbpy), 1338m (νbpy–CH_2O), 1281vs, 1145vs, 1104 vs (νCF_2). HR-MS (FAB): $[M]^+$ $C_{16}N_2H_{14}F_6O_2Pd^{35}Cl_2$ calc. *m*/*z* 555.9371, found 555.9362; $C_{16}N_2H_{14}F_6O_2Pd^{35}Cl^{37}Cl$ calc. *m*/*z* 557.9342, found 557.9349; $C_{16}N_2H_{14}F_6O_2Pd^{37}Cl_2$ calc. *m*/*z* 559.9312, found 559.9316; m.p. = 249 °C.

Analytical data of **4b** (from $[PdCl_2(CH_3CN)_2]$ and ligand **2b**): Yield 96%; ^{1}H NMR (500 MHz, *d*-Me_2SO): δ = 9.10 (2H, s, H-6), 8.56 (2H, d, $^3J_{H-H}$ = 8.2 Hz, H-4), 8.27 (2H, d, $^3J_{H-H}$ = 8.2 Hz, H-3), 4.88 (4H, s, bpy–C**H**$_2$), 4.31 (4H, t, $^3J_{H-H}$ = 14.6 Hz, $CF_2C\mathbf{H}_2$); ^{19}F NMR (470.5 MHz, *d*-Me_2SO): δ = −82.9 (6F, t, $CF_2C\mathbf{F}_3$), −122.9 (4F, m, $CH_2C\mathbf{F}_2$); ^{13}C NMR (126 MHz, *d*-Me_2SO): δ = 70 (bpy–**C**H_2), 66 (bpy–$CH_2O\mathbf{C}H_2$), 109–119 ($\mathbf{C}_2F_5$), 124, 137, 140, 148, 156 (bpy). FT-IR [ν_{max}(KBr)/cm^{-1}]: 1613m, 1477m, 1377m (νbpy), 1196vs, 1137vs, 1104vs (νCF_2). HR-MS (FAB): $[M-Cl]^+$ $C_{18}H_{14}F_{10}N_2O_2Pd^{35}Cl$, calcd *m*/*z* 620.9619, found *m*/*z* 620.9567. $C_{18}H_{14}F_{10}N_2O_2Pd^{37}Cl$, calcd *m*/*z* 622.9589, found *m*/*z* 622.9562; m.p.: decomposed before 355 °C.

4.9. Preparation of Pt complexes, [$PtCl_2$(4,4′-bis($CF_3CH_2OCH_2$)-2,2′-bpy)] (5a) {complex 5a has been recently used as an anticancer drug [11], so its synthesis and cytotoxicity studies have been reported very recently. Reported in this article are its crystallization procedure and its detailed structural studies}

The recrystallization proceeded with dissolution of **5a** in DMF to form first the saturated solution, to which a methanol overlayer (5 mL) was added. Then, solvent diffusion over a period of a week at 25 °C afforded pale yellow crystals of **5a**.

4.10. Preparation of Pt complexes (6a), [$PtBr_2$(5,5′-bis($CF_3CH_2OCH_2$)-2,2′-bpy)] (6a)

Analytical data of **6a** (from $PtBr_2$ and ligand **2a**): Yield 83.8%, orange solid; ^{1}H NMR (500 MHz, *d*-Me_2SO): δ = 9.75 (2H, s, H-6), 8.57 (2H, d, $^3J_{H-H}$ = 8.50 Hz, H-4), 8.35 (2H, d, $^3J_{H-H}$ = 8.50 Hz, H-3), 4.93 (4H, s, bpy–C**H**$_2$), 4.27 (4H, q, $^3J_{H-F}$ = 9.50 Hz, $CF_3C\mathbf{H}_2$). ^{13}C NMR (126 MHz, *d*-Me_2SO): δ 156.4, 148.5, 139.4, 138.1, 124.6 (s, 10C, bpy), 124.6 (q, J_{F-C} = 279.7 Hz, 2 C, –*C*F_3), 70.3 (bpy–**C**H_2), 67.6 (t, bpy–$CH_2O\mathbf{C}H_2$). ^{19}F NMR (470.5 MHz, *d*-Me_2SO): δ −72.7 (6F, s, $CH_2C\mathbf{F}_3$; H-decoupled). FT-IR [ν_{max}(KBr)/cm^{-1}]: 1613m, 1479m,

Table 1
Crystal data and refinement details for compounds of **3a**, **4a**, **5a** and **6a**.

Compound	**3a**	**4a**	**5a**	**6a**
Formula	$C_{16}N_2H_{14}F_6O_2PdCl_2$	$C_{16}N_2H_{14}F_6O_2PdCl_2$	$C_{16}N_2H_{14}F_6O_2PtCl_2$	$C_{16}N_2H_{14}F_6O_2PtBr_2$
M_r	557.59	557.59	646.28	735.20
Crystal systsem	Monoclinic	Triclinic	Monoclinic	Triclinic
Space group	*P* 21/*c*	*P* 21/*c*	*P* 21/*c*	*P*−1
a/Å	9.2180(9)	8.9714(3)	9.274(3)	7.569(0)
b/Å	17.414(2)	30.422(1)	17.393(6)	9.272(1)
c/Å	12.188 (1)	7.1379(2)	12.319(4)	15.042(2)
α/°	90	90	90	93.918(2)
β/°	100.992(4)	92.242(1)	100.352(14)	100.450(2)
γ/°	90	90	90	107.101(2)
V/Å^3	1920.6(3)	1946.6(1)	1954.8(11)	983.9(2)
T/K	200(2)	200(2)	200(2)	200(2)
λ/Å (Mo K)	0.71073	0.71073	0.71073	0.71073
Z	4	4	4	2
D_c/Mg m^{-}3	1.928	1.903	2.196	2.482
μ/mm−1	1.317	1.299	7.522	11.263
F(0 0 0)	1096	1096	1224	684
Range/°	2.25–25.03	1.34–25.03	2.05–25.02	2.78–25.03
Obsd. reflns.	2975	3111	2312	3172
No. param.	262	262	262	262
R, [$I > 2(I)$][a]	0.0286	0.0375	0.0645	0.0282
R_w	0.0712	0. 1140	0.1590	0.0711
GoF	1.054	1.372	1.091	0.810
CCDC no.	791840	791841	84435	84436

[a] Full-matrix least-squares refinement on F^2.

1384m (νbpy), 1273vs, 1183vs, 1126vs (νCF_2). HR-MS (FAB): $C_{16}N_2H_{14}F_6O_2PtBr_2$ calc. *m*/*z* 732.8974, found 732.8964; m.p.: decomposed before 357 °C.

4.11. Single crystal X-ray diffraction studies

The crystal data and structure refinement for Pd complexes, **3a** and **4a**, and Pt complexes, **5a** and **6a**, are listed in Table 1. The diffraction data of **3a**–**6a** were collected at a temperature of 200 K by employing a Bruker CCD diffractometer. The structural refinements were performed with the SHELXL-97 program package. All structures were solved by successive Fourier maps. In the case of **3a**, one molecule exists in the asymmetric unit; however, one of the CF_3 groups is disordered while the other is not. In the case of its analogue, **5a**, one of the CF_3 groups is also disordered.

Acknowledgements

N. Lu thanks for the National Science Council in Taiwan (NSC 98-2113-M-027-002-MY3) for the funding, while J.S. Thrasher thanks The University of Alabama for support.

Appendix A. Supplementary data

CCDC 791840 (a10168), 791841 (a10577), 84435 (a10292) and 84436 (a11092) contain the supplementary crystallographic data for **3a**, **4a**, **5a** and **6a**, respectively. These data can be obtained free of charge via http://www.ccdc.cam.ac.uk/conts/retrieving.html, or from the Cambridge Crystallographic Data Centre, 12 Union Road, Cambridge CB2 1EZ, UK. Fax: +44 1223 336 033; or deposit@ccdc.cam.ac.uk. In addition, supplementary data containing mass spectral studies of bpy ligands can be found, in the online version, at doi:10.1016/j.jfluchem.2012.02.009.

References

[1] J.K. Cho, R. Najman, T.W. Dean, O. Ichihara, C. Muller, M. Bradley, J. Am. Chem. Soc. 128 (2006) 6276–6277.
[2] J. Moineau, G. Pozzi, S. Quici, D. Sinou, Tetrahedron Lett. 40 (1999) 7683–7686.
[3] R.T. Service, Science 330 (2010) 308–309.
[4] G. Poli, G. Giambastiani, A. Heumann, Tetrahedron 56 (2000) 5959–5989.
[5] A. Svennebring, P.J.R. Sjöberg, M. Larhed, P. Nilsson, Tetrahedron 64 (2008) 1808–1812.
[6] N.J. Whitcombe, K.K. Hii, S.E. Gibson, Tetrahedron 57 (2001) 7449–7476.
[7] I.P. Beletskaya, A.V. Cheprakov, Chem. Rev. 100 (2000) 3009–3066.
[8] C.-K. Li, A. Ghalwadkar, N. Lu, J. Organomet. Chem. 696 (2011) 3637–3642.
[9] S.C. Chan, M.C.W. Chan, Y. Wang, C.M. Che, K.K. Cheung, N. Zhu, Chem. Eur. J. 7 (2001) 4180–4190.
[10] K.E. Elwell, C. Hall, S. Tharkar, Y. Giraud, B. Bennett, C. Bae, S.W. Carper, Bioorg. Med. Chem. 14 (2006) 8692–8700.
[11] T.T. Chang, S.V. More, N. Lu, J.-W. Jhuo, Y.-C. Chen, S.-C. Jao, W.-S. Li, Bioorg. Med. Chem. 19 (2011) 4887–4894.
[12] C.Y. Chen, S.J. Wu, C.G. Wu, J.G. Chen, K.C. Ho, Angew. Chem. Int. Ed. 45 (2006) 5822–5825.
[13] J.J. Lagref, M.K. Nazeeruddin, M. Grätzel, Synth. Met. 138 (2003) 333–339.
[14] A.E. Curtright, J.K. McCusker, J. Phys. Chem. A 103 (1999) 7032–7041.
[15] N. Lu, J.-S. Shing, W.-H. Tu, Y.-C. Hsu, J.T. Lin, Inorg. Chem. 50 (2011) 4289–4294.
[16] B.L. Bennett, K.A. Robins, R. Tennant, K. Elwell, F. Ferri, I. Bashta, G. Aguinaldo, J. Fluorine Chem. 127 (2006) 140–145.
[17] L. Murphy, J.A.G. Williams, Top. Organomet. Chem. 28 (2010) 75–111.
[18] G.R.A. Kumara, Langmuir 18 (2002) 10493–10495.
[19] M. Grätzel, Nature 414 (2001) 338–344.
[20] M.K. Nazeeruddin, S.M. Zakeeruddin, J.J. Lagref, P. Liska, P. Comte, C. Barolo, G. Viscardi, K. Schenk, M. Grätzel, Coord. Chem. Rev. 248 (2004) 1317–1328.
[21] S.M. Zakeeruddin, M.K. Nazeeruddin, R. Humphry-Baker, P. Pećhy, P. Quagliotto, C. Barolo, G. Viscard, M. Grätzel, Langmuir 18 (2002) 952–954.
[22] N. Lu, W.H. Tu, Z.W. Wu, Y.S. Wen, L.K. Liu, Acta Crystallogr. C 66 (2010) o289–o291.
[23] N. Lu, W.H. Tu, Y.S. Wen, L.K. Liu, C.Y. Chou, J.C. Jiang, CrystEngComm 12 (2010) 538–542.
[24] N. Lu, H.C. Hou, C.T. Lin, C.K. Li, L.K. Liu, Polyhedron 29 (2010) 1123–1129.
[25] N. Lu, Y.C. Lin, J.Y. Chen, T.C. Chen, S.C. Chen, Y.S. Wen, L.K. Liu, Polyhedron 26 (2007) 3045–3053.
[26] N. Lu, J.Y. Chen, C.W. Fan, Y.C. Lin, Y.S. Wen, L.K. Liu, J. Chin. Chem. Soc. 53 (2006) 1517–1521.
[27] N. Lu, Y.C. Lin, J.Y. Chen, C.W. Fan, L.K. Liu, Tetrahedron 63 (2007) 2019–2023.
[28] N. Lu, Y.C. Lin, Tetrahedron Lett. 48 (2007) 8823–8828.
[29] Y. Akiyama, S. Fujita, X. Meng, Y.C. Chen, N. Lu, F. Zhao, M. Arai, J. Supercrit. Fluids 51 (2009) 209–216.
[30] D.J. Adams, D. Gudmunsen, J. Fawcett, E.G. Hope, A.M. Stuart, Tetrahedron 58 (2002) 3827–3834.
[31] J. Fawcett, E.G. Hope, D.R. Russell, A.M. Stuart, D.R.W. Wood, Polyhedron 20 (2001) 321–326.
[32] P. Bhattacharyya, B. Croxtall, J. Fawcett, J. Fawcett, D. Gudmunsen, E.G. Hope, R.D.W. Kemmitt, D.R. Pagie, D.R. Rusell, A.M. Stuart, D.R.W. Wood, J. Fluorine Chem. 101 (2000) 247–255.
[33] E.G. Hope, R.D.W. Kemmitt, D.R. Paige, A.M. Stuart, D.R.W. Wood, Polyhedron 18 (1999) 2913–2917.
[34] C.S. Consorti, F. Hampel, J.A. Gladysz, Inorg. Chim. Acta 359 (2006) 4874–4884.

[35] S. Quici, M. Cavazzini, S. Ceragioli, F. Montanari, G. Pozzi, Tetrahedron Lett. 40 (1999) 3647–3650.
[36] N. Lu, J.Y. Chen, C.W. Fan, Y.C. Lin, 18th International Symposium on Fluorine Chemistry, Meeting Abstract No. 193, Bremen, Germany, 2006.
[37] N. Lu, Y.C. Lin, Y.Y. Chen, L.K. Liu, J. Chin. Chem. Soc. 55 (2008) 89–96.
[38] R.C. da Costa, F. Hampel, J.A. Gladysz, Polyhedron 26 (2007) 581–588.
[39] N. Lu, W.H. Tu, H.W. Chang, Z.W. Wu, H.C. Su, Acta Crystallogr. E 66 (2011) o355–o356.
[40] A.A. Farah, W.J. Pietro, Polym. Bull. 43 (1999) 135–142.
[41] J.A.K. Howard, V.J. Hoy, D. O'Hagan, G.T. Smith, Tetrahedron 52 (1996) 12613–12622.
[42] B.Z. Momeni, S. Hamzeh, S.S. Hosseini, F. Rominger, Inorg. Chim. Acta 360 (2007) 2661–2668.
[43] B.Z. Momeni, Z. Moradi, M. Rashidi, F. Rominger, Polyhedron 28 (2009) 381–385.
[44] R.H. Herber, M. Croft, M.J. Coyer, B. Bilash, A. Sahinert, Inorg. Chem. 33 (1994) 2422–2426.
[45] V.H. Houlding, V.M. Miskowski, Coord. Chem. Rev. 111 (1991) 145–152.